

A Comparative Study of the DEKF and DUKF for Battery SOC and SOH Estimation

Original

A Comparative Study of the DEKF and DUKF for Battery SOC and SOH Estimation / Seifoddini, Arash; Miretti, Federico; Misul, Daniela Anna. - In: BATTERIES. - ISSN 2313-0105. - ELETTRONICO. - (2025). [10.3390/batteries11110410]

Availability:

This version is available at: 11583/3004935 since: 2025-11-07T07:59:03Z

Publisher:

MDPI

Published

DOI:10.3390/batteries11110410

Terms of use:

This article is made available under terms and conditions as specified in the corresponding bibliographic description in the repository

Publisher copyright

(Article begins on next page)

Study of the thermal distribution for YBCO based Transition Edge Bolometers working above 77 K

Andrea Napolitano, Samuele Ferracin, Michela Fracasso, Roberto Gerbaldo, Gianluca Ghigo, Laura Gozzelino, Daniele Torsello and Francesco Laviano
Dipartimento di Scienza Applicata e Tecnologia (DISAT),
Politecnico di Torino,
Corso Duca degli Abruzzi 24, 10129 Torino, Italy

Andrea Napolitano, Michela Fracasso, Roberto Gerbaldo, Gianluca Ghigo, Laura Gozzelino, Daniele Torsello and Francesco Laviano
INFN, Istituto Nazionale di Fisica Nucleare, Sezione di
Torino,
Via P. Giuria 1, 10125 Torino, Italy

Abstract— Transition Edge Bolometers (TEB) are among the simplest radiation detectors. The straightforward operation mode provides good results only if it is combined with a careful thermal optimization.

In a TEB, the strong dependence of the electrical resistivity on the temperature in its transition zone enables the detection of a variation of the local temperature which can reach tens of μK . For this reason, it is essential to study the thermal profile of the superconducting active part of the detector, hence its substrate, to make it as homogeneous as possible.

Irradiated $\text{YBa}_2\text{Cu}_3\text{O}_{7-x}$ (YBCO) films can be used for position sensitive detection of infrared radiation. A TEB with a double meander pattern, one of which with a reduced critical temperature due to irradiation with high-energy heavy ions, was designed to work in a portable cryostat at a temperature above the liquid nitrogen (LN_2) point.

In this work, we present a series of Finite Element Method simulations (using COMSOL Multiphysics[®]) aimed at the optimization of the thermal distribution above the YBCO film. Once the optimal working point for the device is found, various materials for the bolometer hosting are tested to identify the combination that provides the most homogeneous temperature distribution. The optimal configurations are then analyzed in response to a sudden change in the PID current to determine the one which presents the best behavior in a transient situation.

Keywords—Superconducting bolometer – heavy ions irradiation – YBCO film – COMSOL Multiphysics – Finite element simulation

I. INTRODUCTION

The infrared spectrum presents many interesting applications from space observation to security, from materials control to biomedical imaging [1-4]. However, the devices which present good performance in the THz spectrum are limited [5-6]. Usually, very low operating temperature, below liquid helium, is required to reach high detectivity and low response time. Transition Edge bolometers (TEB) based on High-Temperature Superconductors (HTS) such as $\text{YBa}_2\text{Cu}_3\text{O}_{7-x}$ (YBCO) may overcome both problems exhibiting good performances also above 77K, Liquid Nitrogen (LN_2) boiling point [7-8].

YBCO, being a superconductor, presents a sharp variation in resistance around the critical temperature (T_C) [9]. The transition from the superconductive to the normal state occurs in few Kelvins and the variation in the resistance can reach

values in the order of $\text{k}\Omega/\text{K}$. These characteristics, combined with a good absorbance in the infrared spectrum, make YBCO films an optimal choice for the fabrication of TEBs designed for detecting the THz radiation [10-11].

Because of the TEB high sensibility, these devices can detect variation in the order of fraction of mK. Therefore, it is necessary to maintain the most homogeneous temperature distribution possible along the whole superconducting film.

In this paper, we present the study of the temperature distribution for a YBCO based TEB working in a portable cryostat at a temperature higher than LN_2 . The device is simulated with the software COMSOL Multiphysics[®]. The combination of multiple modules, together with an accurate CAD reproduction and the experimental curve of resistance over temperature, allow us a fine reproduction of the real device [12].

II. DETECTOR STRUCTURE AND DETAIL

A. Portable cryostat

The YBCO bolometer is inserted in a custom-wired dewar (Fig. 1a), which acts as a portable-cryostat that can be filled with LN_2 . The MgO substrate is attached to an aluminum disk equipped with a thermometer. Through a PID control, the system is heated with four SMD (Surface Mounted Device) resistors. The disk is anchored by means of four screws, two of which act as a thermal bridge between the plate and the cold finger. Between the disk and the cold finger is inserted a teflon thermal coupler to reduce the heat transfer. This configuration grants a good thermal distribution and reduces an excessive cooling.

B. Superconducting bolometer

The bolometer under study is made by a 250 nm thick film of YBCO grown by thermal co-evaporation on 0.5 mm thick MgO substrate [13-14]. The superconducting film is patterned using standard photolithography to shape it in a double meander layout. Both meanders are 75 mm long and 35 μm wide and share one voltage pad: this configuration allows us to obtain the voltage drop with a differential measurement and therefore to correct for electro-thermal effects.

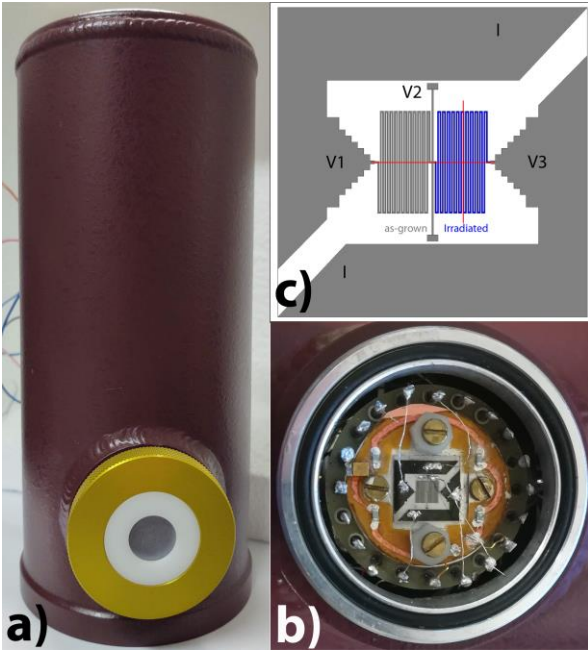


Fig. 1 a) Photo of the portable cryostat which hosts the detector with b) the detail of the double meander detector. c) The electrical scheme for signal detection with the lines over which the temperature profile is analyzed.

One of the two serpentes is irradiated with 114 MeV Au⁺ ions: the strain due to the implantation of the ions in the substrate reduces the T_C increasing the slope of the curve from the superconductive to the normal state [15-17]. The transition of the irradiated meander starts at 83.5 K and the maximum slope is around 10 kΩ/K, while one of the as-grown curve reaches 6.5 kΩ/K, with a T_C of 88 K as shown in Fig. 2.

Exploiting the irradiated meander brings multiple advantages. It allows increasing the responsivity, linked to the slope of the R vs. T curve, and reducing the working temperature and therefore decreasing the noise and the heating power required. Furthermore, the higher T_C of the as-grown meander enables to maintain it in the superconductive state reducing the power consumption and cancelling its contribution to the Johnson noise.

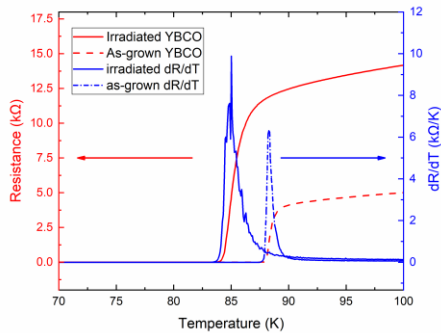


Fig. 2: Resistance versus temperature characterization (left) and its first derivative (right) for both meanders of the YBCO bolometer

C. Working point and theoretical results

To make the most from the TEB it is necessary to find the optimal operating temperature. To do so, a good compromise must be found between the responsivity (1) and noise (2). The first one determines the response of the bolometer as a function of the incoming power, and it is expressed in V/W [18-19]. The noise affects the quality of the measurements and it is the sum of various factors. For this device, the most relevant ones are the Johnson noise, linked to the resistance and the responsivity, and the thermal one, due to the thermal fluctuation.

$$r = \frac{\mu I}{2(G \cdot I^2 \cdot \frac{dR}{dT})} \cdot \frac{dR}{dT} \quad (1)$$

$$NEP^2 = NEP_J^2 + NEP_{th}^2 = 4k_B T^2 G + \frac{4k_B TR}{r^2} \quad (2)$$

In the equations above, μ is the YBCO absorption coefficient, I is the bias current, G is the thermal conductivity of the substrate, dR/dT is the variation of the resistance with temperature, r is the responsivity previously defined, k_B is the Boltzmann constant, T is the operating temperature and R is the resistance of the bolometer.

We investigate these parameters in the range of temperature from 77 K to 88 K, i.e., from the LN₂ temperature to the T_C of the as-grown meander. To find the maximum bias current, the power dissipated from the irradiated meander is kept below 2.5 mW. The maximum responsivity is found at 84.43 K with a bias current of 1.25 mA. With this operating condition, the responsivity is equal to 25 mV/W and the total noise to 75 nW/s^{0.5}. The signal to noise ratio, calculated with a bandwidth of 1 kHz, is higher than 10.

D. Finite Element Modelling with COMSOL Multiphysics®

Different combinations of materials for both sensor holder and screws, reported in the table below, were simulated with COMSOL Multiphysics®.

TABLE 1: MATERIALS COMBINATION UNDER STUDY

Sensor holder	Screws			
	Alluminium	Brass	Copper	Teflon
Alluminium	Alluminium	Brass	Copper	Teflon
Copper	Alluminium	Brass	Copper	Teflon

The CAD of the structure is imported into the FEM software and the physics of the system are meticulously reproduced with thermal and electrical modules. The resistivity and other characteristics of YBCO, such as density and heat transfer coefficient, are taken from experimental measurements.

The radiation mechanism is included, along with thermal conduction. The electric current module is used for the current in the resistor and the differential equation module is used for the PID control. A specific physics for thin layers is chosen to well reproduce both the thermal and the electrical behavior of the YBCO layer. Finally, to take into account the Joule heating and the thermoelectric effects, all those modules are coupled in the multiphysics simulations.

III. THERMAL ANALYSIS

A. Stationary

A first study is performed in a stationary mode: we look for the temperature distribution once the average temperature of the irradiated meander reaches the working value with μK precision. This allows us to make a first material selection according to the thermal homogeneity. The profiles are analyzed in 2D maps to provide a general view and then linear profiles along the x and y-axis are reported to highlight the differences along the irradiated meander. Finally, the higher and lower temperatures reached in the irradiated serpentine are summarized.

The 2D thermal distributions, shown in Fig.3, highlight that just minor differences appear in the choice of the sample holder material while large diversity occurs changing the screw materials, both in final temperature and its distribution.

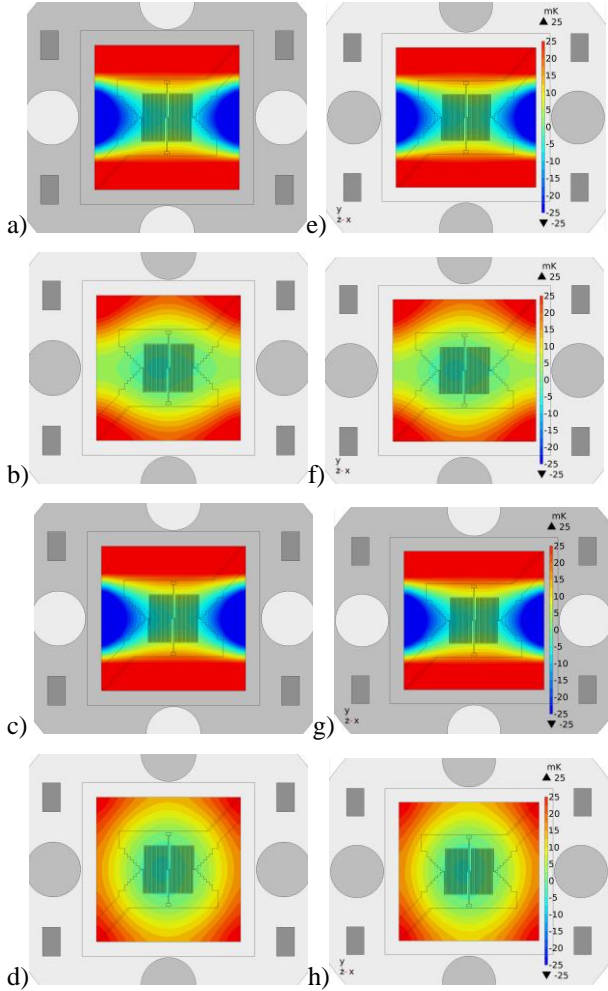


Fig. 3: Differences from the working temperature (84.43 K) distribution for the various combination of materials. On the left, Alluminium sample holder and screws in a) alluminium, b) brass, c) copper and d) teflon. On the right, Copper sample holder and screws in e) alluminium, f) brass, g) copper and h) teflon. The scale is the same for all the graphs.

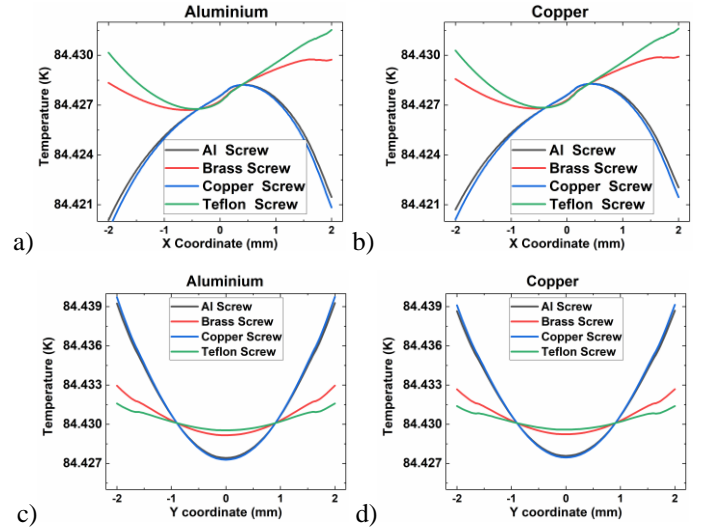


Fig. 4: Linear profiles along the horizontal line traced Fig. 1(c) for the various screw kinds and a) aluminium and b) copper sensor holder and along the vertical line traced Fig. 1(c) for the same screw kinds and c) aluminium and d) copper sensor holder. The similarity between the two sensor holders is evident, while is appreciable the better performance with brass and teflon screws in all the configurations.

The linear profiles, taken in correspondence with the lines displayed in Fig. 1c, are plotted in Fig. 4. It is possible to appreciate the difference between the central and outer part of the meander and the effect of the heat dissipated by the irradiated meander, on the right of Figs. 4a and b. Again, the difference between the two sensor holders is very small while the effect in the selection of the screw material is appreciable.

Finally, the maximum and minimum temperature calculated in the irradiated serpentine, are reported in table 2. Again, the sensor holder material just slightly affects the temperature distribution while the selection of the screw material causes appreciable differences.

TABLE 2: MAXIMUM AND MINIMUM TEMPERATURE AND THEIR DIFFERENCE FOR THE STUDIED CONFIGURATION.

Sensor holder	Screws	Temperature Max [K]	Temperature Min [K]	Temperature difference [mK]
Alluminium	Alluminium	84.436	84.422	13.65
Alluminium	Brass	84.433	84.427	5.52
Alluminium	Copper	84.437	84.422	14.57
Alluminium	Teflon	84.437	84.427	9.15
Copper	Alluminium	84.436	84.423	12.70
Copper	Brass	84.433	84.427	5.37
Copper	Copper	84.436	84.422	13.57
Copper	Teflon	84.433	84.427	5.36

B. Transient

Once that a uniform distribution is found along the superconducting film, the response both to a sudden change in the PID current and to an external signal is studied for the best configuration, i.e., copper for the sensor holder and brass and teflon for the screws. At the beginning of the transient study, we simulate a decrease in the resistors current which fully

recover after 5 seconds. In the same study, 100 seconds the variation in the current, we reproduce an incoming signal modelled as an infrared heat source with a power of 50 W at a distance of 15 cm for 1 ms. In this way, we can investigate the effect of the current variation in the signal detection which happens after a relatively long time. The evolution of the average temperature in the YBCO film for the two configurations, brass and teflon screws, is reported in Fig. 5a, after the current is turned off. A more detailed close up is shown in Fig. 5b. The transient analysis highlights the long time required by the teflon configuration to recover the operating temperature.

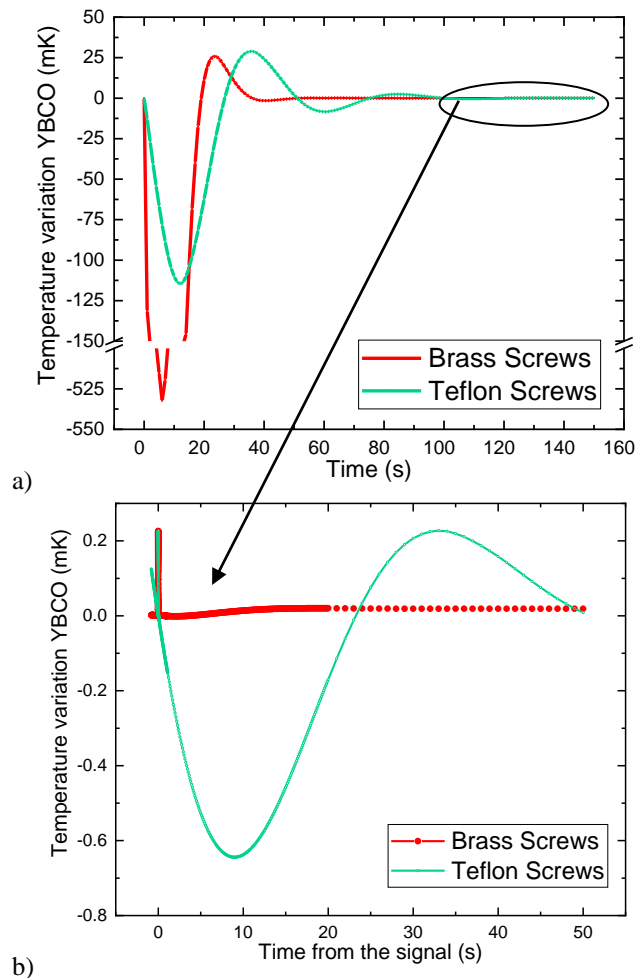


Figure 5: a) Evolution of the YBCO average temperature in response to a loss of current in the resistors. b) Effect of the temperature oscillation in the signal detection after 100 second from the simulated transient. The time in b) is set at 0 in correspondence of the detection of the signal.

IV. CONCLUSION

The use of FEM software for modelling superconducting detector is a useful tool for the design and the optimization of the sensor housing, especially for what concerns thermal distributions. The results obtained allow us to find the best combination of materials for this TEB based on a high-energy heavy-ion irradiated YBCO meander hosted in a portable cryostat. The choice of the sensor holder material just slightly affects the thermal distribution while the selection of the

material of the screws strongly influences it. It is necessary to find a good compromise between high thermal conductance, which does not provide a homogeneous temperature profile, and low one, which provides a slow response to change in temperature. A wider spectrum of materials will be considered, simulated and then experimentally tested in the future.

ACKNOWLEDGMENT

This work was done in the framework of the INFN-TERA project. The staff of INFN-LNL is gratefully acknowledged for support during irradiation experiments.

REFERENCES

- [1] C. Corsi and F. Sizov, eds., THz and Security Applications (Springer Netherlands, 2014).
- [2] A. Ren, et al., "State-of-the-art in terahertz sensing for food and water security – a comprehensive review," *Trends in Food Science & Technology* 85, 241–251 (2019).
- [3] C. Kulesa, "Terahertz spectroscopy for astronomy: From comets to cosmology," *IEEE Transactions on Terahertz Science and Technology* 1, 232–240 (2011).
- [4] Naftaly, Vieweg, and Deninger, "Industrial applications of terahertz sensing: State of play," *Sensors* 19, 4203 (2019).
- [5] P. H. Siegel, "Terahertz technology," in *IEEE Transactions on Microwave Theory and Techniques*, vol. 50, no. 3, pp. 910–928, (March 2002).
- [6] R. A. Lewis *J. Phys. D: Appl. Phys.* 52 433001 (2019).
- [7] R. Mohajeri, R. Nazifi, A. C. Wulff, M. A. Vesaghi, J. Grivel and M. Fardmanesh, "Investigation of CeO₂ Buffer Layer Effects on the Voltage Response of YBCO Transition-Edge Bolometers," in *IEEE Transactions on Applied Superconductivity*, vol. 26, no. 3, pp. 1–4, April 2016, Art no. 2100104.
- [8] R. S. Nebosis, et al., Picosecond YBa₂Cu₃O_{7-δ} detector for far-infrared radiation. *Journal of Applied Physics*, 72(11), 5496–5499 (1992).
- [9] B. Oktem, et al., The superconducting transition width and illumination wavelength dependence of the response of MgO substrate YBCO transition edge bolometers. *Physica C-superconductivity and Its Applications* - 458. 6–11 (2007).
- [10] M. Fardmanesh. Analytic Thermal Modeling for dc-to-Midrange Modulation Frequency Responses of Thin-Film High-Tc Superconductive Edge-Transition Bolometers. *Applied optics*. 40, 2001.
- [11] Mezzetti, E., Gerbaldo, R., Ghigo, G., Gozzelino, L., Laviano, F., Minetti, B., & Rovelli, A., Tuning the absorption band in the THz range of YBCO films patterned by means of HEHI lithography. *Physica C: Superconductivity*, 470(19), 918–921 (2010).
- [12] A. Napolitano et al. *J. Phys.: Conf. Ser.* 1559 012019 (2020).
- [13] B. Utz, R. Semerad, M. Bauer, W. Prusseit, P. Berberich, and H. Kinder, *IEEE Transactions on Applied Superconductivity*, 7 (1997) 1272.
- [14] F. Laviano, et al. Thickness dependence of the current density distribution in superconducting films. *Physica C: Superconductivity*, 404(1–4), 220–225. (2004).
- [15] E. Mezzetti et al., "Localized Photoresponse of YBCO Films Patterned by Heavy-Ion Lithography," in *IEEE Transactions on Applied Superconductivity*, vol. 19, no. 3, pp. 753–756, (June 2009).
- [16] F. Laviano et al. 2010 *Supercond. Sci. Technol.* 23 125008.
- [17] F. Laviano et al., "THz Detection Above 77 K in YBCO Films Patterned by Heavy-Ion Lithography," in *IEEE Sensors Journal*, vol. 10, no. 4, pp. 863–868, April 2010.
- [18] J. C. Mather, "Bolometer noise: nonequilibrium theory," *Appl. Opt.* 21, 1125–1129 (1982).
- [19] M. K. Maul & M. W. P. Strandberg., Equivalent Circuit of a Superconducting Bolometer. *Journal of Applied Physics*, 40(7), 2822–2827 (1969).